


JES

JOURNAL OF
ENVIRONMENTAL
SCIENCES

ISSN 1001-0742
CN 11-2629/X

March 1, 2014 Volume 26 Number 3
www.jesc.ac.cn

Unexpected malformations in
Xenopus tropicalis



Sponsored by
Research Center for Eco-Environmental Sciences
Chinese Academy of Sciences

CONTENTS

Aquatic environment

Metal composition of layered double hydroxides (LDHs) regulating ClO_4^- adsorption to calcined LDHs via the memory effect and hydrogen bonding Yajie Lin, Qile Fang, Baoliang Chen	493
Limitation of spatial distribution of ammonia-oxidizing microorganisms in the Haihe River, China, by heavy metals Chao Wang, Baoqing Shan, Hong Zhang, Yu Zhao	502
Temperature sensitivity of organic compound destruction in SCWO process Yaqin Tan, Zheming Shen, Weimin Guo, Chuang Ouyang, Jinping Jia, Weili Jiang, Haiyun Zhou	512
Influence of moderate pre-oxidation treatment on the physical, chemical and phosphate adsorption properties of iron-containing activated carbon Zhengfang Wang, Mo Shi, Jihua Li, Zheng Zheng	519
Reduction of DOM fractions and their trihalomethane formation potential in surface river water by in-line coagulation with ceramic membrane filtration Pharkphum Rakruam, Suraphong Wattanachira	529
N_2O emission from nitrogen removal via nitrite in oxic-anoxic granular sludge sequencing batch reactor Hong Liang, Jiaoling Yang, Dawen Gao	537
Influence of stabilizers on the antimicrobial properties of silver nanoparticles introduced into natural water Aleksandra Burkowska-But, Grzegorz Sionkowski, Maciej Walczak	542
Addition of hydrogen peroxide for the simultaneous control of bromate and odor during advanced drinking water treatment using ozone Yongjing Wang, Jianwei Yu, Dong Zhang, Min Yang	550
Nitric oxide removal by wastewater bacteria in a biotrickling filter Hejingying Niu, Dennis Y C Leung, Chifang Wong, Tong Zhang, Mayngor Chan, Fred C C Leung	555
Elucidating the removal mechanism of <i>N,N</i> -dimethyldithiocarbamate in an anaerobic-anoxic-oxic activated sludge system Yongmei Li, Xianzhong Cao, Lin Wang	566
Influencing factors of disinfection byproducts formation during chloramination of Cyclops metabolite solutions Xingbin Sun, Lei Sun, Ying Lu, Jing Zhang, Kejing Wang	575

Atmospheric environment

Sources of nitrous and nitric oxides in paddy soils: Nitrification and denitrification Ting Lan, Yong Han, Marco Roelcke, Rolf Nieder, Zucong Cai	581
Upper Yellow River air concentrations of organochlorine pesticides estimated from tree bark, and their relationship with socioeconomic indices Chang He, Jun Jin, Bailin Xiang, Ying Wang, Zhaohui Ma	593
Mechanism and kinetic properties of NO_3 -initiated atmospheric degradation of DDT Cai Liu, Shanqing Li, Rui Gao, Juan Dang, Wenxing Wang, Qingzhu Zhang	601
Sorption and phase distribution of ethanol and butanol blended gasoline vapours in the vadose zone after release Ejikeme Ugwoha, John M. Andresen	608

Terrestrial environment

Effects of temperature change and tree species composition on N_2O and NO emissions in acidic forest soils of subtropical China Yi Cheng, Jing Wang, Shenqiang Wang, Zucong Cai, Lei Wang	617
---	-----

Environmental biology

Influence of sunlight on the proliferation of cyanobacterial blooms and its potential applications in Lake Taihu, China Qichao Zhou, Wei Chen, Kun Shan, Lingling Zheng, Lirong Song	626
Bioavailability and tissue distribution of Dechloranes in wild frogs (<i>Rana limnocharis</i>) from an e-waste recycling area in Southeast China Long Li, Wenyue Wang, Quanxia Lv, Yujie Ben, Xinghong Li	636

Environmental health and toxicology

Unexpected phenotypes of malformations induced in <i>Xenopus tropicalis</i> embryos by combined exposure to triphenyltin and 9- <i>cis</i> -retinoic acid Jingmin Zhu, Lin Yu, Lijiao Wu, Lingling Hu, Huahong Shi	643
Expression of sulfur uptake assimilation-related genes in response to cadmium, bensulfuron-methyl and their co-contamination in rice roots Jian Zhou, Zegang Wang, Zhiwei Huang, Chao Lu, Zhuo Han, Jianfeng Zhang, Huimin Jiang, Cailin Ge, Juncheng Yang	650

Environmental catalysis and materials

Reaction mechanism and metal ion transformation in photocatalytic ozonation of phenol and oxalic acid with Ag^+/TiO_2
Yingying Chen, Yongbing Xie, Jun Yang, Hongbin Cao, Yi Zhang 662

Effect of TiO_2 calcination temperature on the photocatalytic oxidation of gaseous NH_3
Hongmin Wu, Jinzhu Ma, Changbin Zhang, Hong He 673

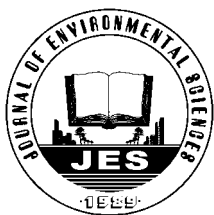
Effects of synthesis methods on the performance of $\text{Pt} + \text{Rh}/\text{Ce}_{0.6}\text{Zr}_{0.4}\text{O}_2$ three-way catalysts
Zongcheng Zhan, Liyun Song, Xiaojun Liu, Jiao Jiao, Jinzhou Li, Hong He 683

Catalytic combustion of soot over ceria-zinc mixed oxides catalysts supported onto cordierite
Leandro Fontanetti Nascimento, Renata Figueredo Martins, Rodrigo Ferreira Silva, Osvaldo Antonio Serra 694

Effects of metal and acidic sites on the reaction by-products of butyl acetate oxidation over palladium-based catalysts
Lin Yue, Chi He, Zhengping Hao, Shunbing Wang, Hailin Wang 702

Mechanism of enhanced removal of quinonic intermediates during electrochemical oxidation of Orange II under ultraviolet irradiation
Fazhan Li, Guoting Li, Xiwang Zhang 708

Serial parameter: CN 11-2629/X*1989*m*223*en*P*26*2014-3

Available online at www.sciencedirect.com

Journal of Environmental Sciences

www.jesc.ac.cn

Metal composition of layered double hydroxides (LDHs) regulating ClO_4^- adsorption to calcined LDHs via the memory effect and hydrogen bonding

Yajie Lin^{1,2}, Qile Fang^{1,2}, Baoliang Chen^{1,2,*}1. Department of Environmental Science, Zhejiang University, Hangzhou 310058, China. E-mail: yjlin90@163.com

2. Zhejiang Provincial Key Laboratory of Organic Pollution Process and Control, Hangzhou 310058, China

ARTICLE INFO

Article history:

Received 14 October 2013

revised 25 November 2013

accepted 18 December 2013

Keywords:

calcined layered double hydroxides

perchlorate

adsorption memory effect

hydrogen bonds

DOI: 10.1016/S1001-0742(13)60462-3

ABSTRACT

A series of calcined carbonate layered double hydroxides (CLDHs) with various metal compositions and different $\text{M}^{2+}/\text{M}^{3+}$ ratios were prepared as adsorbents for perchlorate. Adsorption isotherms fit Langmuir model well, and the adsorption amount followed the order of $\text{MgAl-CLDHs} \geq \text{MgFe-CLDHs} \gg \text{ZnAl-CLDHs}$. The isotherms of MgAl-CLDHs and MgFe-CLDHs displayed a two-step shape at low and high concentration ranges and increased with an increase in the $\text{M}^{2+}/\text{M}^{3+}$ ratio from 2 to 4. The two-step isotherm was not observed for ZnAl-CLDHs , and the adsorption was minimally affected by the $\text{M}^{2+}/\text{M}^{3+}$ ratio. The LDHs, CLDHs and the reconstructed samples were characterized by X-ray diffraction, SEM, FT-IR and Raman spectra to delineate the analysis of perchlorate adsorption mechanisms. The perchlorate adsorption of MgAl-CLDHs and MgFe-CLDHs was dominated by the structural memory effect and the hydrogen bonds between the free hydroxyl groups on the reconstructed-LDHs and the oxygen atoms of the perchlorates. For ZnAl-CLDHs , the perchlorate adsorption was controlled by the structural memory effect only, as the hydroxyl groups on the hydroxide layers preferred to form strong hydrogen bonds with carbonate over perchlorate, which locked the intercalated perchlorate into a more confined nano-interlayer. Several distinct binding mechanisms of perchlorate by CLDHs with unique M^{2+} ions were proposed.

Introduction

Layered double hydroxides (LDHs) have been increasingly considered to function as novel functional materials to control environmental pollution, especially for organic and inorganic anionic pollutants (Goh et al., 2008; Lin et al., 2014). LDHs are characterized by positively charged layer structures, due to the isomorphous substitution of M^{2+} to M^{3+} (Cavani et al., 1991; Khan and O'Hare, 2002; Rives and Ulibarri, 1999). In the formula $[\text{M}_{1-x}\text{M}_x^{3+}(\text{OH})_2]^{x+}(\text{A}^{n-})_{x/h} \cdot m\text{H}_2\text{O}$, the type of M^{2+} , M^{3+} , A^{n-} and the value of x ($x = \text{M}^{3+}/(\text{M}^{2+} + \text{M}^{3+})$) can be changed as needed (Allmann et al., 1970; Cavani et al., 1991; Duan and Evans, 2006; Rives and Ulibarri,

1999). This flexibility made LDHs popular in many fields. For example, the change of the x value could affect the purity of LDHs, and the distance between M^{2+} and M^{3+} could cause a change in the layer charge density (Newman et al., 2001; Sideris et al., 2008). The types of M^{2+} and M^{3+} would affect the unit cell parameters, following a change of interlayer spacing such as spatial symmetry or spacing distance (Gregoire et al., 2012; Wang et al., 2008; Yan et al., 2009). These features will eventually impact the molecular mechanism between the hydroxide layer and the interlayer anion, which further determine the environmental applications of LDHs (Kloprogge et al., 2002; Lin et al., 2014; Miyata, 1980).

The calcined carbonate LDHs (CLDHs) are prepared as novel adsorbents for the abatement of anionic pollutants from aqueous solution, and they are dominated by the structural reconstruction of LDHs (i.e., memory effect)

* Corresponding author. E-mail: blchen@zju.edu.cn

(Cai et al., 2012; Lin et al., 2014; Rocha et al., 1999; Lv et al., 2006). In the majority of previous studies, on the anion adsorption of LDHs and CLDHs, have focused on the anions' adsorption performance on LDHs under various environmental conditions (Goh and Lim 2010; Sandip et al., 2013; Wang et al., 2008; Zhang et al., 2012). However, few reports on the molecular interactions between anions and LDHs or CLDHs are available, though it is of paramount importance to accurately predict the adsorptive properties of the adsorbent and subsequently to optimize the adsorption and regeneration processes (Goh et al., 2012; Wang et al., 2008). Goh and Lim (2010) completed an excellent work on the interaction mechanisms of oxyanions and oxyhalides that have different molecular properties on Mg/Al LDHs nanoparticles. The monovalent oxyhalides (BrO_3^- , ClO_3^- , IO_3^- , and ClO_4^-) were adsorbed by LDHs mainly via the anion exchange mechanism with subsequent formation of outer-sphere surface complexes. Comparatively, the polyvalent oxyanions (HAsO_4^{2-} , $\text{B}_2\text{O}_7^{2-}$, CrO_4^{2-} , MoO_4^{2-} , and VO_4^{3-}) were associated with LDHs via both anion exchange and ligand exchange reactions, which resulted in the coexistence of both outer-sphere and inner-sphere surface complexes (Goh et al., 2012).

Perchlorate (ClO_4^-) is an emerging trace contaminant with a tetrahedron structure (Fang and Chen, 2012; Jackson et al., 2010; McDougal et al., 2011). As the chlorine atom (in the center of the tetrahedron structure) is surrounded by four oxygen atoms, the perchlorate ion exhibits strong stability and refractory properties (Kirk, 2006; Motzer, 2001). Thus, it is viewed as a persistent environmental pollutant (Fang et al., 2011). Furthermore, when it enters the human body, it may cause metabolic disturbance and thus induce a series of diseases (Roy and Bickerton, 2012; Lv et al., 2006; Wilkin et al., 2007; Fang and Chen, 2013). Certain studies regarding the application of LDHs to remove perchlorate mainly focused on the removal capacity because of their higher adsorption capacity than many other adsorbents (Kim et al., 2011; Lien et al., 2010; Seliem et al., 2011; Xu et al., 2010; Yang et al., 2012). However, the specific interaction mechanism of perchlorate with LDHs should be elucidated at molecular levels. Furthermore, the regulating roles of the flexible structure of LDHs in the interaction mechanisms have yet to be determined.

The main objective of this work was to probe the molecular interaction mechanisms of perchlorate with CLDHs by changing the composition types and ratios of $\text{M}^{2+}/\text{M}^{3+}$ on the CLDHs. We hypothesize that the different metal compositions may impact the content, site, and orientation of the hydroxyl groups in the LDHs, which directly affect the H-bond formation and regulate their contribution to perchlorate uptake. To this end, $\text{Mg}^{2+}/\text{Al}^{3+}$, $\text{Mg}^{2+}/\text{Fe}^{3+}$ and $\text{Zn}^{2+}/\text{Al}^{3+}$ carbonate LDHs with molar ratios of 2, 3 and 4 were synthesized, and corresponding CLDHs

were prepared. The adsorption of perchlorate to CLDHs was performed by the batch equilibration method. To explain the analysis of the interaction mechanism, X-ray diffraction (XRD), scanning electron microscopy (SEM), Fourier transform infrared spectroscopy (FT-IR) and Raman spectra were applied for the characterization of the carbonate LDHs, CLDHs, and the reconstructed associated ClO_4^- ions of the LDH samples.

1 Experimental

1.1 Synthesis of LDHs and CLDHs.

A series of carbonate MgAl-LDHs, MgFe-LDHs, and ZnAl-LDHs with $\text{M}^{2+}/\text{M}^{3+}$ molar ratios of 2, 3 and 4, respectively, were synthesized using a conventional co-precipitation method described elsewhere (Lin et al., 2014). In detail, solution A was prepared by dissolving $\text{MCl}_2 \cdot 6\text{H}_2\text{O}$ and $\text{MCl}_3 \cdot 6\text{H}_2\text{O}$ in 200 mL of DI water, and the total concentration of $\text{M}^{2+} + \text{M}^{3+}$ was 2 mol/L. Solution B was mixed with NaOH and Na_2CO_3 in 200 mL of DI water, yielding concentrations of 2 mol/L NaOH and 0.2 mol/L Na_2CO_3 . All of the chemicals used were of analytical grade. A peristaltic pump was used to add the two solutions to a 500 mL conical flask, and the rate was regulated at 1 drop per second. The conical flask was placed in a water bath with vigorous magnetic stirring at room temperature. After the two solutions underwent homogeneous mixing, the conical flask was kept still for the precipitate aged at 75°C. The precipitation was then collected, washed with repeat centrifugation and dried at 65°C. The CLDHs were obtained from the LDHs in a muffle furnace at 500°C for 3 hr. The selected temperature was the most favorable calcination temperature range, which was widely used to prepare CLDHs using the memory effect (Lv et al., 2006; Yang et al., 2012). The obtained solid was ground and passed through a 0.154 mm sieve. The final LDHs were named with MgAl-LDHs-2, MgAl-LDHs-3, and MgAl-LDHs-4 for the LDHs with Mg/Al ratios of 2, 3, and 4, respectively. The corresponding CLDHs were named MgAl-CLDHs-2, MgAl-CLDHs-3, and MgAl-CLDHs-4. Similarly, the sample names of MgAl-LDHs, MgAl-CLDHs, MgFe-LDHs, MgFe-CLDHs, ZnAl-LDHs, and ZnAl-CLDHs were changed according to the metal composition instead of MgAl, MgFe, and ZnAl.

1.2 Sorption experiments

The batch equilibration method was applied to the adsorption isotherms of perchlorate using different CLDHs. The natural pH of the LDH suspension was 10. Each isotherm contained fourteen concentration points ranging from 1 to 450 mg/L, including the blank samples and parallel samples. A given amount of CLDHs were added

to the glass screw-cap vials with different concentrations of ClO_4^- . When apparent equilibrium was obtained by shaking the solid-liquid mixture at 25°C and 120 r/min for 24 hr, the solid was separated by centrifugation. The filtered supernatant was analyzed using ion chromatography (IC system ICS1500, Dionex) which was equipped with a Dionex 4-mm ASRS suppressor, 4×250 mm IonPac AS16 column, 4×50 mm IonPac AG16 guard column and a twenty-five-microliter injection loop. The detection was operated under a 60 mmol/L NaOH eluent flowing at 1 mL/min at 30°C, and the detection limit of perchlorate was 0.05 mg/L. The reconstructed LDHs with ClO_4^- as an interlayer anion were named MgAl-LDHs- ClO_4^- , MgFe-LDHs- ClO_4^- , and ZnAl-LDHs- ClO_4^- .

1.3 Structural characterization of samples before and after the adsorption of perchlorate

The structures of the carbonate LDHs, CLDHs and the reconstructed LDHs after the adsorption of perchlorate ions were characterized by XRD, SEM, FT-IR and Raman. The XRD patterns were obtained by a Rigaku D/Max 2550/PC diffractometer with Cu $K\alpha$ radiation ($\lambda = 1.541 \text{ \AA}$) at a scanning rate of $2^\circ/\text{min}$ and a step size of 0.02° – 0.05° of 2θ . The SEM images were shot by a field emission scanning electron microscope manufactured by FEI SIRON in Holland. The FT-IR spectra were collected using a Bruker Vector 22 FT-IR spectrophotometer, using KBr pellets at a resolution of 1.0 cm^{-1} with a scan range

of 4000 – 400 cm^{-1} . The Raman spectra were recorded through a LabRAM HR UV instrument, equipped with an Olympus microscope, triple monochromator and a Peltier-cooled charge-coupled device. An Ar^+ laser (514.5 nm) that excited at a resolution of 1.0 cm^{-1} was applied to produce relevant spectra.

2 Results and discussion

2.1 Structural characteristics of LDHs and CLDHs

The XRD patterns of the carbonate LDHs and the CLDH are shown in **Fig. 1**. The distinct reflections of (003), (006), (012), (015), (018) and (110) in the LDHs- CO_3 patterns indicated the formation of the typical lamellae structure (Duan and Evans, 2006; Newman et al., 2001; Rocha et al., 1999). Only hydrotalcite phase was observed in each sample, and no crystalline phase was detected. The presence of (012), (015) and (018) reflections suggested that the LDHs have the $3R_1$ structure, which always appeared in LDHs- CO_3 (Duan et al., 2006). The patterns of CLDHs only showed the metal oxide diffraction peaks. The cell parameter c , calculated from the d_{003} value ($c = 3d_{003}$), corresponds to the adjacent distance of the hydroxide layer; the parameter a , calculated from the d_{110} value ($a = 2d_{110}$), corresponds to the average distance between the M^{2+} and M^{3+} cations within the layers (Cavani et al.,

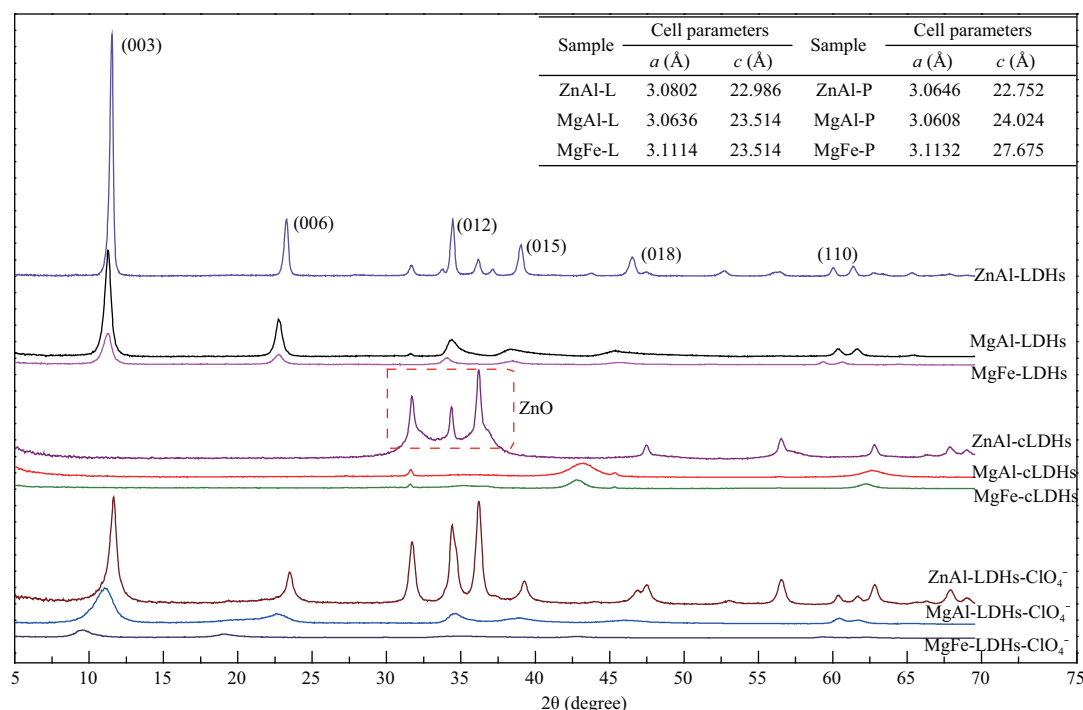


Fig. 1 X-ray diffraction patterns of the LDHs- CO_3 , CLDH samples and the reconstructed LDHs samples after adsorbing ClO_4^- with different metal cation composition (ZnAl, MgAl, and MgFe). The inserted table presents the lattice (unit cell) parameters, in which the a value corresponds to the average distance between the M^{2+} and M^{3+} cations within the layers, and the c value refers to three times the layer-to-layer distance, assuming a $3R_1$ stacking of the layers. The molar ratio of $\text{M}^{2+}/\text{M}^{3+}$ equals 3.

1991). These parameters of the LDH- CO_3 are listed in the inserted table in **Fig. 1**. The value of a for MgAl-LDH-3 (i.e., 0.306 nm) was smaller than the value for ZnAl-LDH-3 (i.e. 0.308 nm) because the Shannon crystal radius of Mg^{2+} (0.086 nm) is smaller than that of Zn^{2+} (0.088 nm). Similarly, the value of a for MgAl-LDH-3 was less than that of MgFe-LDH-3 (i.e. 0.311 nm) because the crystal radius of Al^{3+} (0.0675 nm) was lower than that of Fe^{3+} (0.0785 nm) (Shannon, 1976). The parameter c value appears to be more dependent on the type of M^{2+} over the type of M^{3+} . For example, the c value of ZnAl-LDH-3 (2.299 nm) was smaller than that of MgAl-LDH-3, while both MgAl-LDH-3 and MgFe-LDH-3 have a similar value of the c parameter (2.351 nm). Interestingly, the Shannon crystal radius of Zn^{2+} (0.088 nm) was larger than Mg^{2+} (0.086 nm), but the adjacent distance of the hydroxide layer (i.e. c) of ZnAl-LDH-3 was smaller than that of MgAl-LDH-3, suggesting that the carbonate anions in the ZnAl-LDHs interlayer displayed tighter assembly with the brucite-like layer, which may be difficult for other anions to exchange. Similarly, the Shannon crystal radius of Fe^{3+} was larger than that of Al^{3+} , but MgAl-LDH-3 and MgFe-LDH-3 have a similar c value because the replacement of Al^{3+} by Fe^{3+} in LDHs strengthens the bond between the double-hydroxide layers and carbonates in the interlayer by increasing the positive surface charge (Yang et al., 2012).

The selected SEM images of ZnAl-LDH-3 and MgAl-LDH-3 samples are displayed in **Fig. 2**. It is clear that the particles of the ZnAl-LDHs were larger than the MgAl-LDH particles, which may be attributed to the strong interaction between the hydroxide layers bound to Zn^{2+} and the subsequent aggregation of LDHs into larger particles. The images clearly showed a hexagonal shape for ZnAl-LDH-3 and a staggered appearance of ZnAl-CLDH-3, which are consistent with the LDHs and CLDHs reported (Allmann, 1970). Note that the MgFe-LDH and MgFe-CLDH samples were not characterized by SEM, as these samples display very strong magnetic properties.

The FT-IR spectra of the LDHs- CO_3 and CLDHs samples were presented in **Fig. S1**. The carbonate LDHs have two remarkable peaks at 1364 and 1638 cm^{-1} , and a broad peak ranging from 3400 to 3600 cm^{-1} , which is ascribed to the anti-symmetric stretching vibration of C–O, the stretching vibration of C=O, and the stretching modes of the O–H groups in the hydroxide layer and water molecules, respectively. The large width of the band at 3400–3600 cm^{-1} indicated that hydrogen bonds existed within a broad range of strengths (Goh et al., 2012; Yang et al., 2012). The peak at 3475 cm^{-1} was assigned to the stretching vibration of hydrogen-bonded groups in the brucite-like sheets and water in the interlayer space. When the characteristic peak of the hydroxyl groups evolved from a low wave number (3475 cm^{-1}) to a high wave number (3560 cm^{-1}), the hydroxyl groups changed from a

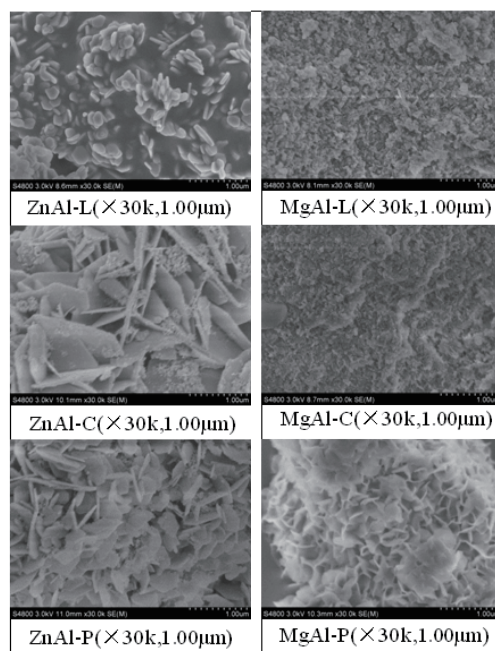


Fig. 2 Selected SEM images of the LDHs- CO_3 , CLDHs, and the reconstructed LDHs- ClO_4 with Zn/Al and Mg/Al as metal cations. “L” stands for LDHs, “C” stands for CLDHs, and “P” stands for the reconstructed samples after adsorbing ClO_4^- . The molar ratio of $\text{M}^{2+}/\text{M}^{3+}$ equals 3.

hydrogen bond state to free hydroxyl groups (Costa et al., 2010). Reasonably, the height ratios of the two hydroxyl peaks at high and low wave number (i.e. $I_{\text{high}}/I_{\text{low}}$) can be used as an indicator of the existence of free hydroxyl groups. The calculated $I_{\text{high}}/I_{\text{low}}$ ratios were 0, 0.815 and 0.968 for ZnAl-LDH-3, MgFe-LDH-3 and MgAl-LDH-3, respectively, which indicate that the MgAl-LDHs particles contain a higher content of free hydroxyl groups than that of MgFe-LDHs particles, and there are no free hydroxyl groups in the ZnAl-LDH particles. Presumably, the free hydroxyl groups act as the potential binding sites for the interlayer anions and may play an important role in the adsorption characteristics and interaction mechanisms of LDHs or CLDHs with anions.

2.2 Adsorption properties of perchlorate by CLDHs

The adsorption isotherms of perchlorate onto the MgAl-CLDHs, MgFe-CLDHs and ZnAl-CLDHs with different molar ratios of $\text{M}^{2+}/\text{M}^{3+}$ are presented in **Fig. 3**. The adsorption isotherms fit Langmuir equation well, and the regression parameters are listed in **Table 1**. It is obvious that the adsorption of perchlorate by CLDHs is significantly affected by the metal compositions and the molar ratios of $\text{M}^{2+}/\text{M}^{3+}$. For LDHs at 2 molar ratios of $\text{M}^{2+}/\text{M}^{3+}$, the saturated adsorption capacity in the magnitude followed the order of MgAl-CLDH-2 (65.61 mg/g) \approx MgFe-CLDH-2 (65.61 mg/g) \gg ZnAl-CLDH-2 (8.56 mg/g), while for the molar ratios of $\text{M}^{2+}/\text{M}^{3+}$ at 4, MgAl-CLDH-4 (279.6

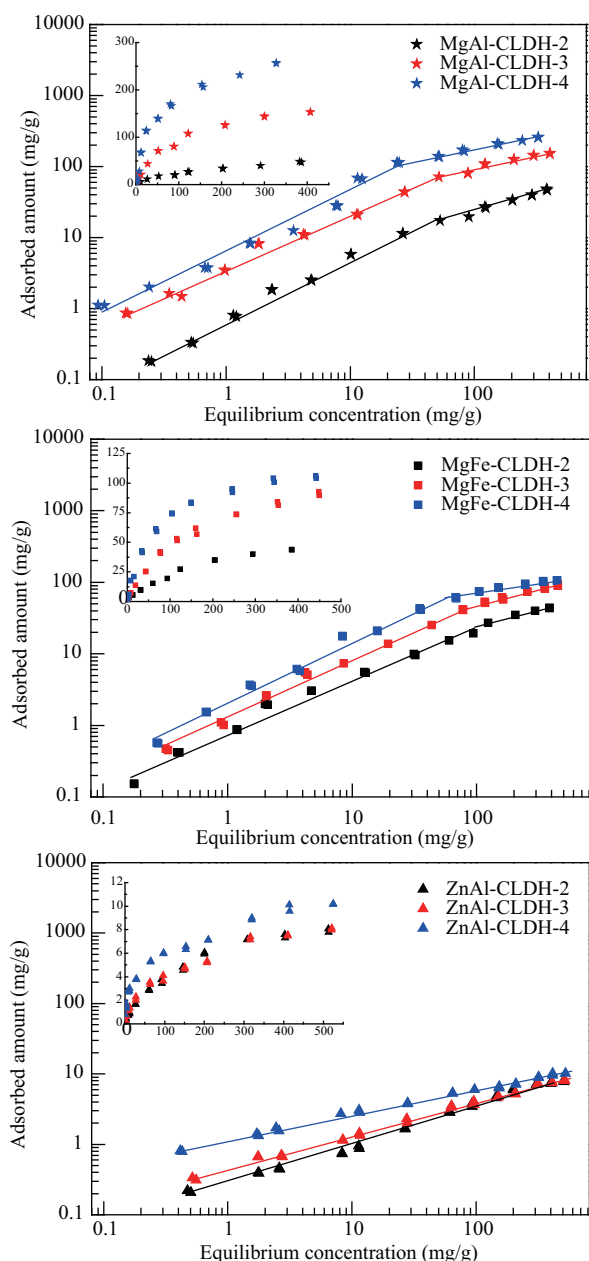


Fig. 3 Adsorption isotherms of ClO_4^- onto CLDHs with different metal cation composition and molar ratios.

mg/g) > MgFe-CLDH-4 (120.8 mg/g) \gg ZnAl-CLDH-4 (10.81 mg/g). Similar studies indicated that the adsorption of fluoride (F^-) to CLDHs was dependent on the influences of metal cations in the LDH layers (Duan et al., 2006). The retention of fluoride by MgAl-CLDH was higher than that of ZnAl-CLDH, which is partly due to the lower anion exchange capacity of ZnAl-CLDH. Although F^- in the previous (Duan et al., 2006) and ClO_4^- in the current study have different anion structures, the same phenomenon of MgAl-CLDH > ZnAl-CLDH is observed.

Based on **Fig. 3** and **Table 1**, for the MgAl-CLDHs groups, the adsorption capacity of perchlorate increased with increasing $\text{M}^{2+}/\text{M}^{3+}$ ratio from 2 to 4. For the MgFe-

CLDHs groups, the saturated adsorption amount increased with the $\text{M}^{2+}/\text{M}^{3+}$ ratio from 2 to 3 and then leveled off at 4. For the ZnAl-CLDHs groups, the adsorption capacity was almost invariant with the $\text{M}^{2+}/\text{M}^{3+}$ ratio. Recently, the effects of a varying Mg/Al molar ratio on the removal of fluoride by CLDHs were reported (Duan et al., 2006). However, the retention of fluoride by the CLDH with a Mg/Al molar ratio of 2 was the best one (reached 80 mg/g) and larger than that of fluoride by the CLDH with Mg/Al ratios of 3 and 4, which was explained by the higher charge density in the layers of CLDH with an Mg/Al ratio of 2. The distinct impacts of the Mg/Al molar ratio on the adsorption of F^- (reverse) and ClO_4^- (positive) to CLDHs suggested that additional adsorption mechanisms besides the memory effect may be involved in ClO_4^- binding. In the current study, the influencing degree of the ratio of the metal cations on the perchlorate adsorption to CLDHs is dependent on the metal cation compositions, which indicated that the additional mechanism can be regulated by both metal cation ratios and metal composition.

The Langmuir parameter b values presented in **Table 1** correspond to the affinity between the absorbency of CLDHs and the adsorbency of perchlorate. For MgAl-CLDHs and MgFe-CLDHs, the b values increased with the molar ratio of $\text{M}^{2+}/\text{M}^{3+}$, while for ZnAl-CLDHs, the b values decreased with the $\text{M}^{2+}/\text{M}^{3+}$ molar ratio. Thus, an unusual adsorption mechanism may take place when the ZnAl-CLDHs band perchlorate from aqueous solution, which are distinct from the MgAl-CLDHs and MgFe-CLDHs groups. Furthermore, when the adsorption isotherms were fitted with the Freundlich equation, an inflection point was observed in the whole isotherm for the MgAl-CLDHs and MgFe-CLDHs groups (**Fig. 3**), but not for the ZnAl-CLDHs group. The Freundlich regression parameters at low and high concentration ranges for the MgFe-CLDHs groups are presented in **Table S1**. The results indicate that there may be two recognizable interaction mechanisms contributing to the binding of perchlorate to MgAl-CLDHs and MgFe-CLDHs in the low and high concentration ranges, while only one interaction mechanism in the tested concentrations can be discernible for the ZnAl-CLDHs.

2.3 Perchlorate uptake by CLDHs with memory effect

CLDHs were demonstrated to recover their original layered structure in the presence of perchlorate, which is the so-called "memory effect". The memory effect was identified by the XRD patterns (**Fig. 1**). That is, the feature diffraction peaks of (003), (006), (012), (015), (018) and (110), which refer to the lamellae structure of LDHs, disappeared after calcined to CLDHs, and then recovered after the ClO_4^- adsorption process. Furthermore, the SEM images of LDHs, CLDHs and the reconstructed LDHs associated with perchlorate (**Fig. 2**), directly supported the memory effect, but the recovering degree was dis-

Table 1 Langmuir regression parameters of ClO_4^- adsorption isotherms onto CLDHs with different $\text{M}^{2+}/\text{M}^{3+}$ molar ratios ^a

Metal cation	$\text{M}^{2+}/\text{M}^{3+}$ molar ratio	Q^0 (mg/g)	b (L/mg)	R^2
MgAl-CLDH	2	65.61 ± 3.39	0.0057 ± 0.0006	0.988
	3	186.6 ± 4.2	0.0105 ± 0.0007	0.955
	4	279.6 ± 7.4	0.0212 ± 0.0018	0.990
MgFe-CLDH	2	65.61 ± 2.26	0.0053 ± 0.0004	0.995
	3	120.8 ± 1.4	0.0063 ± 0.0003	0.998
	4	120.8 ± 2.4	0.0149 ± 0.0006	0.998
ZnAl-CLDH	2	8.56 ± 0.17	0.0584 ± 0.0060	0.975
	3	9.82 ± 0.52	0.0075 ± 0.0011	0.970
	4	10.81 ± 0.32	0.0058 ± 0.0004	0.994

^a The Langmuir parameters (Q^0 and b) were calculated using the form of the equation $Q = Q^0 b C_e / (1 + b C_e)$, where Q^0 (mg/g) is the Langmuir capacity coefficient, b (L/mg) is the adsorption rate coefficient, and C_e (mg/L) is equilibrium concentration.

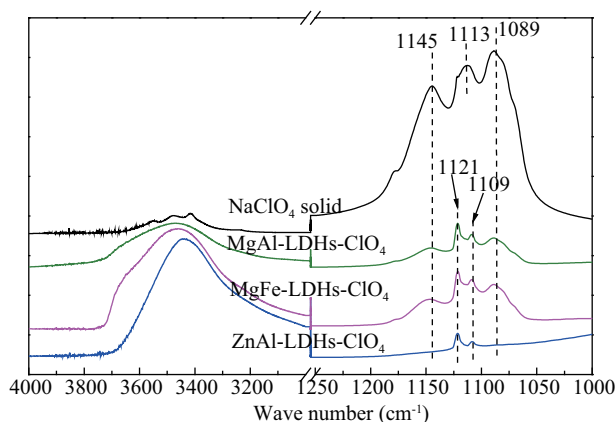


Fig. 4 FT-IR spectra of the solid NaClO_4 and the reconstructed LDHs- ClO_4 ($\text{M}^{2+}/\text{M}^{3+}$ molar ratio of 3). The hydroxyl group characteristic peak ranged from 4000–3000 cm^{-1} . The characteristic perchlorate peak of the O-Cl vibration ranged from 1250–1000 cm^{-1} .

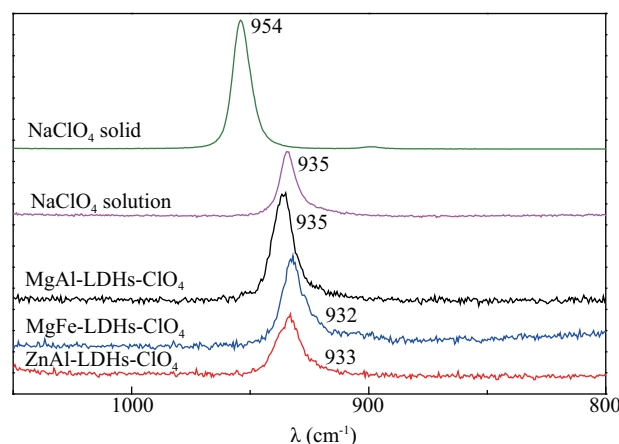


Fig. 5 Raman spectra of the NaClO_4 solid, NaClO_4 solution, and the reconstructed LDHs- ClO_4 with different metal cations. The molar ratio of $\text{M}^{2+}/\text{M}^{3+}$ equals 3.

tinct for the CLDHs samples with different metal cation composition. The perchlorate characteristic peaks in the FT-IR spectra (**Fig. 4**) and the Raman spectra (**Fig. 5**) for the LDHs- ClO_4 provided powerful evidence for the intercalation of ClO_4^- in the interlayer of the reconstructed LDHs. A previous study of the removal of fluoride by MgAl-CLDH indicated that the adsorption phenomenon was accompanied by rehydration with concomitant uptake of fluoride ions to rebuild the initial layered structure (Duan et al., 2006).

The different memory effect phenomena were observed for MgAl-CLDHs, MgFe-CLDHs and ZnAl-CLDHs. Firstly, the ZnAl-CLDHs displayed an obvious ZnO diffraction peak in **Fig. 1**, and the ZnO diffraction peak still remained when other lamellar diffraction peaks recovered after the adsorption process of perchlorate, which demonstrates the incomplete recovery of the samples. Moreover, the SEM images of ZnAl-LDHs- ClO_4 showed many staggers such as the CLDHs, reflecting the incomplete recovery to the lamellar feature of LDHs. When LDHs- CO_3 was changed to LDHs- ClO_4 , the ZnAl-LDHs

showed a decrease in the cell parameter c from 2.299 to 2.275 nm, but an increase of parameters c from 2.351 to 2.402 nm for the MgAl group was observed. The increase of parameter c for the MgAl-LDHs was caused by the higher ion radius of ClO_4^- (0.292 nm) than CO_3^{2-} (0.266 nm), while the decrease of parameter c for the ZnAl-LDHs may be caused by the strong interaction between the interlayer anions and the hydroxide layer.

The XRD spectra of MgFe-CLDHs in **Fig. S2** explained that the memory effect is effective in the adsorption process, as the recovery of the lamellar diffraction peaks. However, the diffraction peaks of (012), (015) and (018), which represent the $3R_1$ structure of the interlayer, had disappeared, indicating the change of the interlayer space of LDHs. In the FT-IR spectra (**Fig. S1**) with the M-O characteristic vibration peaks approximately 600 cm^{-1} , significant change occurred when the LDHs calcined to the CLDHs, and the M-O vibration peak in the LDHs- ClO_4 spectrum could not be recovered to the similar vibration peak as the LDHs- CO_3 spectrum due to the formation of the Fe_3O_4 phase. These may be the major reasons for the

great enlargement of the cell parameter c value from 2.351 nm for MgFe-LDHs- CO_3 to 2.768 nm for MgFe-LDHs- ClO_4 . The change in the c value (0.416 nm) was eight times higher than the change for MgAl-LDHs of 0.0510 nm (from 2.351 nm for MgAl-LDHs- CO_3 to 2.402 nm for MgAl-LDHs- ClO_4).

2.4 Adsorption mechanism of perchlorate to CLDHs with different metal compositions

The adsorption mechanisms of the anions by LDHs and CLDHs have been increasingly concerning to optimize their environmental applications (Cai et al., 2012; Goh et al., 2010, 2012). Goh et al. (2012) suggested that monovalent oxyhalides (BrO_3^- , ClO_3^- , IO_3^- , and ClO_4^-) were adsorbed to LDHs via the anion exchange process (an electrostatic Coulombic interaction) following the formation of outer sphere complexes, while the polyvalent oxyanions (HAsO_4^{2-} , $\text{B}_2\text{O}_7^{2-}$, CrO_4^{2-} , MoO_4^{2-} , SeO_4^{2-} , and VO_4^{3-}) were adsorbed on LDHs by forming inner-sphere bidentate surface complexes. The sorption reaction of arsenate with the LDHs occurred through two mechanisms, i.e. primary anion exchange mechanism and secondary ligand exchange mechanism (Goh et al., 2010). In this study, the adsorption of perchlorate by CLDHs was mainly driven by the structural memory effect with perchlorate as an interlayer anion to rebuild the LDHs' structure (Goh et al., 2012), and hydrogen bonds between hydroxyl groups of hydroxide layer and oxygen atom of perchlorate were proposed as an additional mechanism to favor perchlorate adsorption. Furthermore, the existing states of perchlorate in the nano-interlayer of the reconstructed LDHs were characterized by FT-IR and Raman spectra to elucidate the effect of metal cations on the adsorption mechanism of perchlorate via the memory effect and hydrogen bonding. Distinct binding mechanisms of perchlorate by CLDHs with unique M^{2+} are proposed in Fig. 6. The Cl–O vibration in perchlorate and the O–H vibration in LDHs vibration are very sensitive to probe the surrounding environments in the interlayer spacing of LDHs, which consist of different metal cations. The Raman spectra of solid NaClO_4 , aqueous NaClO_4 , and the reconstructed LDHs with perchlorate as an interlayer anion are presented in Fig. 5. The Cl–O vibrations of the LDHs- ClO_4^- (932–935 cm^{-1}) are close to the ClO_4^- in liquid form (935 cm^{-1}) rather than the solid form (954 cm^{-1}), which suggested that the ClO_4^- in the LDHs were surrounded by hydroxyl groups other than interaction with positively charged groups by electrostatic attraction.

In Fig. 4, the differences between the four Cl–O vibrations in the FT-IR spectra reflect the different existing states of ClO_4^- (Ha and Kim, 2011) in the interlayer of the reconstructed LDHs. The existence state of perchlorate in the interlayer spacing of reconstructed MgAl-LDHs- ClO_4^- and MgFe-LDHs- ClO_4^- were almost the same, demonstrated by the FT-IR spectra. When perchlorate was intercalated into the interlayer of MgFe-CLDH and presented as MgFe-

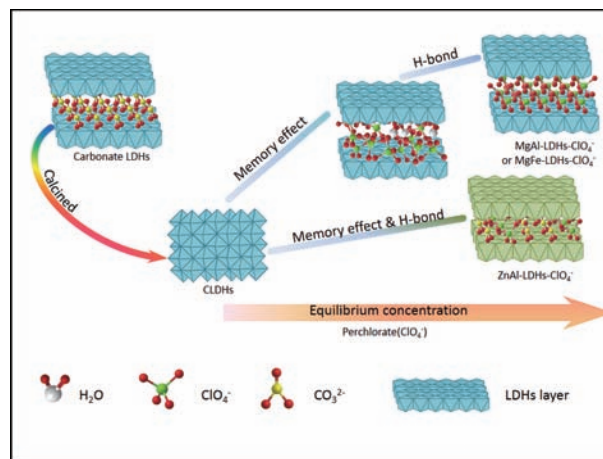


Fig. 6 Schematic of perchlorate adsorption by CLDHs. The memory effect and hydrogen bonds are regulated by the metal cations' composition. For MgAl-CLDHs and MgFe-CLDHs, the contribution of the memory effect and hydrogen bonds can be differentiated by the perchlorate concentrations, which is not the case for ZnAl-CLDHs.

LDHs- ClO_4 , two Cl–O vibrations at 1145 and 1089 cm^{-1} were weakened and broadened for the restriction in the limited interlayer spacing, and the two overlap vibrations of Cl–O at 1112 cm^{-1} in the perchlorate solid were divided into two distinct peaks at 1121 and 1109 cm^{-1} mainly due to the electron density redistribution. The vibrational peak of the hydroxyl at a high wave number (3560 cm^{-1}) illustrated that the free hydroxyl groups are rich in the MgFe-LDHs- ClO_4 interlayer, which may serve as adsorptive sites for the intercalated perchlorate. In addition, the lower adsorption capacity of perchlorate on MgFe-CLDHs in contrast to MgAl-CLDHs is attributed to two reasons. One is the lower hydroxyl peak ratio ($I_{\text{high}}/I_{\text{low}}$) for MgFe-LDHs than MgAl-LDHs, which led to the reduction of the availability of the hydroxyl groups for binding anions. The other reason may be ascribed to a break in the interlayer $3R_1$ symmetry structure in the MgFe-LDHs- ClO_4 which blocks the intercalation of perchlorate into the interlayer spacing; the enlargement of interlayer spacing also induces the unstable connection between the perchlorate and hydroxyl groups. For the MgFe-CLDHs sample, the adsorption character is quite similar to the MgAl-CLDHs, and their adsorption processes were performed in two steps. These suggest that the two interaction mechanisms originated from the memory effect with electrostatic attraction, and hydrogen bonds can be differentiated in MgAl-CLDHs and MgFe-CLDHs via regulating perchlorate concentrations, which are schematically described in Fig. 6.

For the ZnAl-CLDH samples, the adsorption mechanism was distinct from the MgAl-CLDH and MgFe-CLDHs (Fig. 6). For the reconstructed ZnAl-LDHs- ClO_4 , the carbonate characteristic vibration peak at 1364 cm^{-1} still remained in the FT-IR spectrum (Fig. S1). From

Fig. 1, the (006) reflection peak of the ZnAl-LDHs in the XRD pattern was assigned to the carbonate phase, which was still presented in the ZnAl-LDHs-ClO₄ as a distinct and sharp peak. These indicate that both the carbonate and perchlorate anions were intercalated into the interlayer of LDHs as complementary anions via the memory effect. To contrast, only little or no carbonate could be observed in the reconstructed MgAl-LDHs-ClO₄ and MgFe-LDHs-ClO₄ samples. In the FT-IR spectrum of ZnAl-LDHs-ClO₄ (**Fig. 4**), the two Cl–O vibrations at 1145 and 1089 cm^{−1} disappeared, and the other two Cl–O vibration peaks at 1121 and 1109 cm^{−1} were very weak, demonstrating that the perchlorate is seriously restricted in the interlayer spacing of ZnAl-LDHs-ClO₄. Note that only one peak at a low wave number approximately 3475 cm^{−1} was observed for the hydroxyl characteristic vibration in the ZnAl-LDHs-CO₃ and ZnAl-LDHs-ClO₄, which are ascribed to the hydroxyl groups in the ZnAl-LDHs, all involved in hydrogen bonds (Chiang and Wu, 2011). The strong interaction of carbonate with the hydroxyl groups in the hydroxide layer of ZnAl-LDHs via hydrogen bonding make no free hydroxyl groups available for more anions. Therefore, ZnAl-CLDHs display more preferential binding with carbonate over perchlorate in aqueous solution. The value of the Langmuir parameter *b* for ZnAl-CLDHs decreased with an increase in the Zn²⁺/Al³⁺ molar ratio. In other words, the affinity of perchlorate to ZnAl-CLDHs increased with an increase in the hydroxide layer charge density, i.e., the higher the charge density of the CLDHs, the higher the affinity to the anions, which assumes that electrostatic interaction plays a dominant role in the perchlorate adsorption process by ZnAl-CLDHs. Although the anion radius of carbonate (0.266 nm) is significantly smaller than that of perchlorate (0.292 nm), the interlayer spacing of ZnAl-LDHs-CO₃ (*c* = 2.299 nm) was larger than the reconstructed ZnAl-LDHs-ClO₄. These usual phenomena suggest that in addition to being interlayer anions, the intercalated perchlorate still serves as a hydrogen bond donor to strongly interact with the hydroxyl groups as hydrogen bond acceptors located in the hydroxide layer of the ZnAl-LDHs-ClO₄. The strong hydrogen bonds between the anions and the hydroxyl groups make perchlorate extremely restricted in the interlayer, which was proven by the Cl–O characteristic vibration in the FT-IR spectra. For ZnAl-CLDH, the adsorption of perchlorate is mostly performed by the memory effect, but the adsorption capacity of perchlorate is very weak due to the competition of carbonate. The memory effect and hydrogen bonds contribute to perchlorate binding in the interlayer of ZnAl-CLDHs, but they can be distinguished by the perchlorate concentrations (**Fig. 6**) due to the lack of free hydroxyl groups and limited interlayer space.

3 Conclusions

The structural characteristics, perchlorate adsorption properties and binding mechanisms of the calcined carbonate layered double hydroxides (CLDHs) are dependent on the metal cation compositions (MgAl, MgFe and ZnAl) and the molar M²⁺/M³⁺ ratio. The binding mechanisms of perchlorate by CLDHs are much more dependent on the unique M²⁺ compared to the type of M³⁺. Adsorption isotherms fit well with the Langmuir model, and the adsorption amount followed the order of MgAl-CLDHs ≥ MgFe-CLDHs >> ZnAl-CLDHs. The isotherms of MgAl-CLDHs and MgFe-CLDHs displayed a two-step shape at low and high concentration ranges and increased with an increase in the M²⁺/M³⁺ ratio from 2 to 4. For ZnAl-CLDHs, however, the two-step isotherms were not observed, and the adsorption was hardly affected by the M²⁺/M³⁺ ratio. The perchlorate adsorption mechanisms of MgAl-CLDHs and MgFe-CLDHs were dominated by the memory effect and hydrogen bonds, which can be differentiated via regulating perchlorate concentrations. To contrast, the perchlorate adsorption by ZnAl-CLDHs was controlled by the memory effect only, as the hydroxyl groups on the hydroxide layers preferred to form strong hydrogen bonds with carbonate rather than perchlorate. The memory effect and hydrogen bonds that contributed to the perchlorate adsorption by ZnAl-CLDHs cannot be distinguished by the perchlorate concentrations due to the lack of free hydroxyl groups and limited interlayer spacing.

Acknowledgments

This work was supported by the National Natural Science Foundation of China (No. 41071210), the Zhejiang Provincial Natural Science Foundation of China (No. R5100105), and the Doctoral Fund of Ministry of Education China (No. J20130039).

Supplementary materials

The supplementary data associated with this study can be found in the online version.

REFERENCES

- Allmann, R., 1970. Double layer structures with layer ions (Me(II)_(1-x)Me(III)_(x)(OH)₂)^(x+) of brucite type. *Chimia*. 24(3): 99.
- Cai, P., Zheng, H., Wang, C., Ma, H.W., Hu, J.C., Pu, Y.B. et al., 2012. Competitive adsorption characteristics of fluoride and phosphate on calcined Mg-Al-CO₃ layered double hydroxides. *J. Hazard. Mater.* 213, 100–108.
- Cavani, F., Trifiro, F., Vaccari, A., 1991. Hydrotalcite-type anionic clays: preparation properties and applications. *Catal. Today* 11(2), 173–301.
- Chiang, M.F., Wu, T.M., 2011. Intercalation of γ-PGA in Mg/Al layered double hydroxides: An *in situ* WAXD and FTIR investigation.

- Appl. Clay. Sci. 51(3), 330–334.
- Costa, D.G., Rocha, A.B., Diniz, R., Souza, W.F., Chiaro, S.S., Leitao, A.A., 2010. Structural model proposition and thermodynamic and vibrational analysis of hydrotalcite-like compounds by DFT calculations. *J. Phys. Chem. C* 114(33), 14133–14140.
- Duan, X., Evans, D.G., 2006. Layered Double Hydroxides: Structure and Bonding. Springer, Berlin/Heidelberg. 119: 1–87.
- Fang, Q.L., Chen, B.L., 2011. A review of phyto-microbial remediation of perchlorate-contaminated soil and groundwater. *Acta Scientiae Circumstantiae* 31(8), 1569–1579.
- Fang, Q.L., Chen, B.L., 2012. Natural origins, formation mechanisms, and fate of environmental perchlorate. *Prog. Chem.* 24(10), 2040–2053.
- Fang, Q.L., Chen, B.L., 2013. Environmental transport behaviors of perchlorate as an emerging pollutant and their effects on food safety and health risk. *Chin. Sci. Bull.* 58(26), 2626–2642.
- Goh, K.H., Lim, T.T., 2010. Influences of co-existing species on the sorption of toxic oxyanions from aqueous solution by nanocrystalline Mg/Al layered double hydroxide. *J. Hazard. Mater.* 180(1–3), 401–408.
- Goh, K.H., Lim, T.T., Banas, A., Dong, Z.L., 2012. Sorption characteristics and mechanisms of oxyanions and oxyhalides having different molecular properties on Mg/Al layered double hydroxide nanoparticles. *J. Hazard. Mater.* 179(1–3), 818–827.
- Goh, K.H., Lim, T.T., Dong, Z., 2008. Application of layered double hydroxides for removal of oxyanions: A review. *Water Res.* 42(6–7), 1343–1368.
- Gregoire, B., Ruby, C., Carteret, C., 2012. Structural cohesion of M^{II} - M^{III} layered double hydroxides crystals: Electrostatic forces and cationic polarizing power. *Cryst. Growth. Des.* 12(9), 4324–4333.
- Ha, J.H., Kim, J., 2011. Perchlorate anion on manganese(III) porphyrin as an ATR-IR probe for nanoscopic water environments. *Chem. Phys. Lett.* 502(1–3), 92–95.
- Jackson, W.A., Bohlke, J.K., Gu, B.H., Hatzinger, P.B., Sturchio, N.C., 2010. Isotopic composition and origin of indigenous natural perchlorate and co-occurring nitrate in the southwestern United States. *Environ. Sci. Technol.* 44(13), 4869–4876.
- Khan, A.I., O'Hare, D., 2002. Intercalation chemistry of layered double hydroxides: Recent developments and applications. *J. Mater. Chem.* 12(11), 3191–3198.
- Kim, J.Y., Komarneni, S., Parette, R., Cannon, F., Katsuki, H., 2011. Perchlorate uptake by synthetic layered double hydroxides and organo-clay minerals. *Appl. Clay. Sci.* 51(1–2), 158–164.
- Kirk, A.B., 2006. Environmental perchlorate: Why it matters? *Anal. Chim. Acta* 567(1), 4–12.
- Kloprogge, J.T., Wharton, D., Hickey, L., Frost, R.L., 2002. Infrared and Raman study of interlayer anions CO_3^{2-} , NO_3^- , SO_4^{2-} and ClO_4^- in Mg/Al-hydrotalcite. *Am. Mineral.* 87(5–6), 623–629.
- Lien, H.L., Yu, C.C., Lee, Y.C., 2010. Perchlorate removal by acidified zero-valent aluminum and aluminum hydroxide. *Chemosphere* 80(8), 888–893.
- Lin, Y.J., Fang, Q.L., Chen, B.L., 2014. Perchlorate uptake and molecular mechanisms by magnesium/aluminum carbonate layered double hydroxides and calcined layered double hydroxides. *Chem. Eng. J.* 237, 38–46.
- Lv, L., He, J., Wei, M., Evans, D.G., Duan, X., 2006. Factors influencing the removal of fluoride from aqueous solution by calcined Mg-Al- CO_3 layered double hydroxides. *J. Hazard. Mater.* 133(1–3), 119–128.
- McDougal, J.N., Jones, K.L., Fatuyi, B., Gray, K.J., Blount, B.C., Valentin-Blasini, L. et al., 2011. The effects of perchlorate on thyroidal gene expression are different from the effects of iodide deficiency. *J. Toxicol. Env. Heal. A* 74(14), 917–926.
- Miyata, S., 1980. Physicochemical properties of synthetic hydrotalcites in relation to composition. *Clay. Clay. Miner.* 28(1), 50–56.
- Motzer, W.E., 2001. Perchlorate: Problems, detection, and solutions. *Environ. Forensics* 2(4), 301–311.
- Newman, S.P., Greenwell, H.C., Coveney, P.V., Jones, W., 2001. Layered Double Hydroxides: Present and Future. Nova Science, New York.
- Rives, V., Ulibarri, M.A., 1999. Layered double hydroxides (LDH) intercalated with metal coordination compounds and oxometalates. *Coordin. Chem. Rev.* 181(1), 61–120.
- Rocha, J., del Arco, M., Rives, V., Ulibarri, M.A., 1999. Reconstruction of layered double hydroxides from calcined precursors: A powder XRD and ^{27}Al MAS NMR study. *J. Mater. Chem.* 9(10), 2499–2503.
- Roy, J.W., Bickerton, G., 2012. Toxic groundwater contaminants: An overlooked contributor to urban stream syndrome? *Environ. Sci. Technol.* 46(2), 729–736.
- Sandip, M., Swagatika, T., Tapswani, P., Manoj, K.S., Raj, K.P., 2013. Removal efficiency of fluoride by novel Mg-Cr-Cl layered double hydroxide by batch process from water. *J. Env. Sci.* 25(5), 993–1000.
- Seliem, M.K., Komarneni, S., Parette, R., Katsuki, H., Cannon, F.S., Shahien, M.G., et al., 2011. Perchlorate uptake by organosilicas, organo-clay minerals and composites of rice husk with MCM-48. *Appl. Clay. Sci.* 53(4), 621–626.
- Shannon, R.D., 1976. Revised effective ionic-radii and systematic studies of interatomic distances in halides and chalcogenides. *Acta. Crystallogr. A* 32, 751–767.
- Sideris, P.J., Nielsen, U.G., Gan, Z.H., Grey, C.P., 2008. Mg/Al ordering in layered double hydroxides revealed by multinuclear NMR spectroscopy. *Science* 321(5885), 113–117.
- Wang, S.L., Liu, C.H., Wang, M.K., Chuang, Y.H., Chiang, P.N., 2008. Arsenate adsorption by Mg/Al- NO_3 layered double hydroxides with varying the Mg/Al ratio. *Appl. Clay. Sci.* 43(1), 79–85.
- Wilkin, R.T., Fine, D.D., Burnett, N.G., 2007. Perchlorate behavior in a municipal lake following fireworks displays. *Environ. Sci. Technol.* 41(11), 3966–3971.
- Xu, J.H., Gao, N.Y., Tang, Y.L., Deng, Y., Sui, M.H., 2010. Perchlorate removal using granular activated carbon supported iron compounds: Synthesis, characterization and reactivity. *J. Env. Sci.* 22(11), 1807–1813.
- Yan, H., Wei, M., Ma, J., Li, F., Evans, D.G., Duan, X., 2009. Theoretical study on the structural properties and relative stability of M(II)-Al layered double hydroxides based on a cluster model. *J. Phys. Chem. A* 113(21), 6133–6141.
- Yang, Y.Q., Gao, N.Y., Chu, W.H., Zhang, Y.J., Ma, Y., 2012. Adsorption of perchlorate from aqueous solution by the calcination product of Mg/(Al-Fe) hydrotalcite-like compounds. *J. Hazard. Mater.* 209, 318–325.
- Zhang, J., Li, Y., Zhou, J.Z., Chen, D., Qian, G.R., 2012. Chromium(VI) and zinc(II) waste water co-treatment by forming layered double hydroxides: Mechanism discussion via two different processes and application in real plating water. *J. Hazard. Mater.* 205–206, 111–117.

Table S1 Freundlich regression parameters of ClO_4^- adsorption isotherms under low concentration and high concentration ranges onto MgFe-CLDH with different molar ratios of metal cations ^a

CLDHs	Low concentration range			High concentration range		
	$\lg K_f$	N	R^2	$\lg K_f$	N	R^2
CLDH-2	-0.1077 ± 0.0272	0.7449 ± 0.0238	0.983	0.2551 ± 0.1118	0.5446 ± 0.0487	0.932
CLDH-3	0.1046 ± 0.0202	0.8103 ± 0.0185	0.992	0.7883 ± 0.0353	0.4442 ± 0.0153	0.987
CLDH-4	0.3114 ± 0.0251	0.8768 ± 0.0286	0.986	1.1173 ± 0.0501	0.3546 ± 0.0228	0.949

^a The Freundlich parameters (K_f and N) were calculated using the form of the equation $\lg Q = \lg K_f + N \lg C_e$, where Q is the amount adsorbed per unit weight of sorbent, mg/kg; C_e is the equilibrium concentration of the aqueous phase, mg/L; K_f [(mg/g)/(mg/L) ^{N}] is the Freundlich capacity coefficient, and N describes the isotherm curvature. R^2 is regression coefficient.

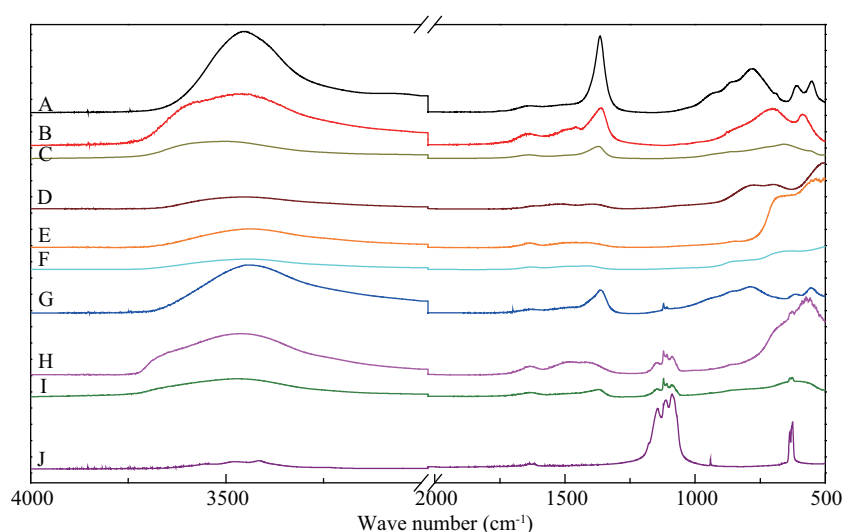
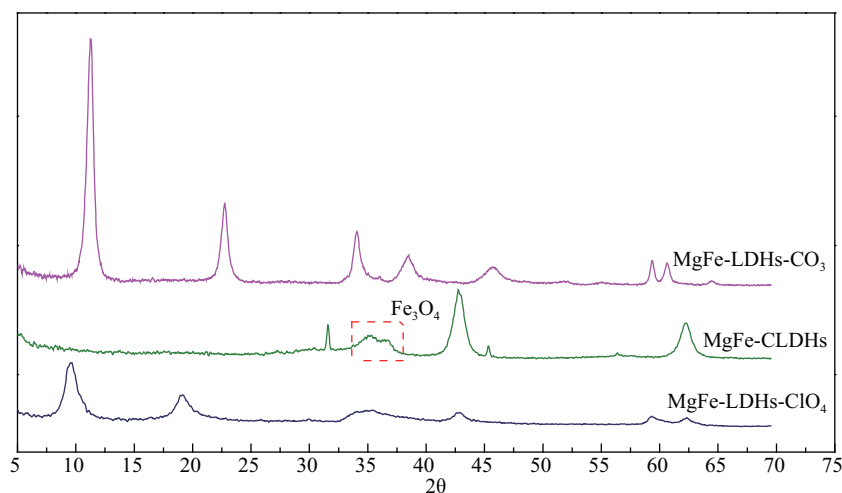
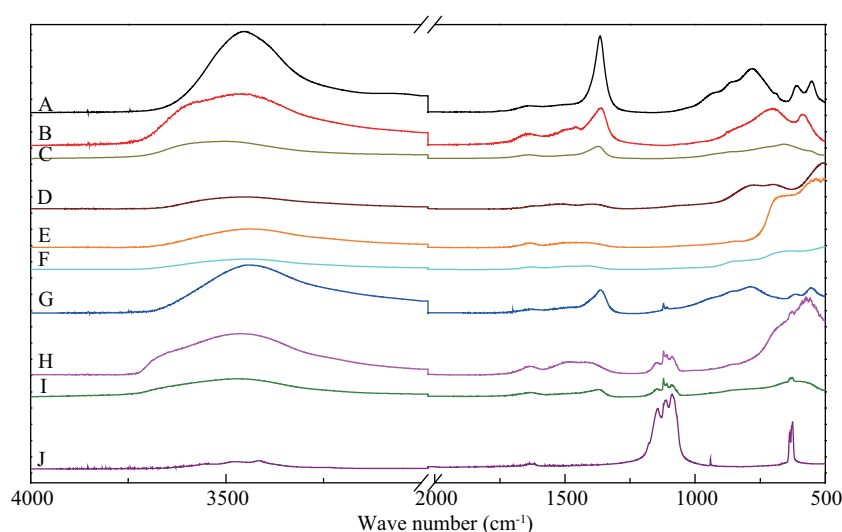
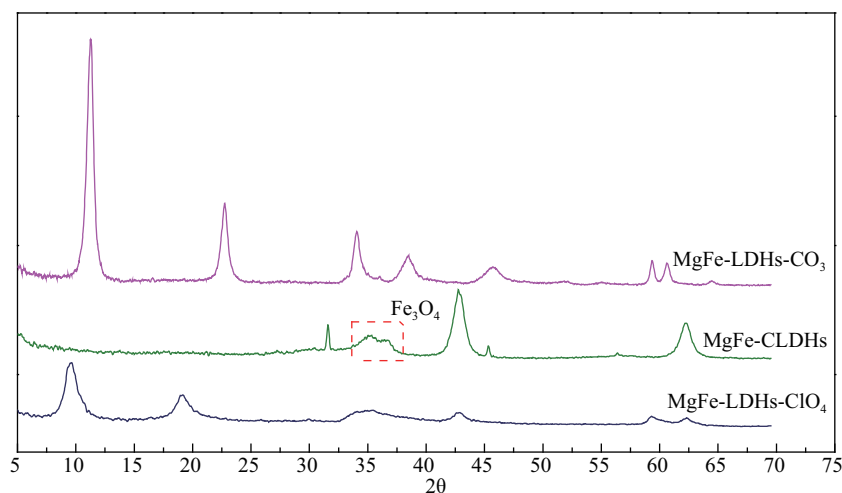
**Fig. S1** FT-IR spectra of the LDHs, CLDHs and the reconstructed LDHs- ClO_4^- . The symbols A, B and C refer to ZnAl-LDH, MgFe-LDH and MgAl-LDH. The symbols D, E and F refer to ZnAl-CLDH, MgFe-CLDH and MgAl-CLDH. The symbols G, H and I refer to the reconstructed ZnAl-LDH- ClO_4 , MgFe-LDH- ClO_4 and MgAl-LDH- ClO_4 . The symbol J corresponds to solid NaClO_4 . The metal ratio of $\text{M}^{2+}/\text{M}^{3+}$ equals 3 in all of the samples.**Fig. S2** XRD spectra of MgFe-LDHs- CO_3 , MgFe-CLDHs and the reconstructed MgFe-LDH- ClO_4 . The molar ratio of $\text{Mg}^{2+}/\text{Al}^{3+}$ equals 3.

Table S1 Freundlich regression parameters of ClO_4^- adsorption isotherms under low concentration and high concentration ranges onto MgFe-CLDH with different molar ratios of metal cations ^a

CLDHs	Low concentration range			High concentration range		
	$\lg K_f$	N	R^2	$\lg K_f$	N	R^2
CLDH-2	-0.1077 ± 0.0272	0.7449 ± 0.0238	0.983	0.2551 ± 0.1118	0.5446 ± 0.0487	0.932
CLDH-3	0.1046 ± 0.0202	0.8103 ± 0.0185	0.992	0.7883 ± 0.0353	0.4442 ± 0.0153	0.987
CLDH-4	0.3114 ± 0.0251	0.8768 ± 0.0286	0.986	1.1173 ± 0.0501	0.3546 ± 0.0228	0.949

^a The Freundlich parameters (K_f and N) were calculated using the form of the equation $\lg Q = \lg K_f + N \lg C_e$, where Q is the amount adsorbed per unit weight of sorbent, mg/kg; C_e is the equilibrium concentration of the aqueous phase, mg/L; K_f [(mg/g)/(mg/L) ^{N}] is the Freundlich capacity coefficient, and N describes the isotherm curvature. R^2 is regression coefficient.

**Fig. S1** FT-IR spectra of the LDHs, CLDHs and the reconstructed LDHs- ClO_4^- . The symbols A, B and C refer to ZnAl-LDH, MgFe-LDH and MgAl-LDH. The symbols D, E and F refer to ZnAl-CLDH, MgFe-CLDH and MgAl-CLDH. The symbols G, H and I refer to the reconstructed ZnAl-LDH- ClO_4 , MgFe-LDH- ClO_4 and MgAl-LDH- ClO_4 . The symbol J corresponds to solid NaClO_4 . The metal ratio of $\text{M}^{2+}/\text{M}^{3+}$ equals 3 in all of the samples.**Fig. S2** XRD spectra of MgFe-LDHs- CO_3 , MgFe-CLDHs and the reconstructed MgFe-LDH- ClO_4 . The molar ratio of $\text{Mg}^{2+}/\text{Al}^{3+}$ equals 3.



Editorial Board of Journal of Environmental Sciences

Editor-in-Chief

Hongxiao Tang Research Center for Eco-Environmental Sciences, Chinese Academy of Sciences, China

Associate Editors-in-Chief

Jiuhui Qu Research Center for Eco-Environmental Sciences, Chinese Academy of Sciences, China
Shu Tao Peking University, China
Nigel Bell Imperial College London, United Kingdom
Po-Keung Wong The Chinese University of Hong Kong, Hong Kong, China

Editorial Board

Aquatic environment

Baoyu Gao
Shandong University, China
Maohong Fan
University of Wyoming, USA
Chihpin Huang
National Chiao Tung University
Taiwan, China
Ng Wun Jern
Nanyang Environment &
Water Research Institute, Singapore
Clark C. K. Liu
University of Hawaii at Manoa, USA
Hokyoung Shon
University of Technology, Sydney, Australia
Zijian Wang
Research Center for Eco-Environmental Sciences,
Chinese Academy of Sciences, China
Zhiwu Wang
The Ohio State University, USA
Yuxiang Wang
Queen's University, Canada
Min Yang
Research Center for Eco-Environmental Sciences,
Chinese Academy of Sciences, China
Zhifeng Yang
Beijing Normal University, China
Han-Qing Yu
University of Science & Technology of China

Terrestrial environment

Christopher Anderson
Massey University, New Zealand
Zucong Cai
Nanjing Normal University, China
Xinbin Feng
Institute of Geochemistry,
Chinese Academy of Sciences, China
Hongqing Hu
Huazhong Agricultural University, China
Kin-Che Lam
The Chinese University of Hong Kong
Hong Kong, China
Erwin Klumpp
Research Centre Juelich, Agrosphere Institute
Germany
Peijun Li
Institute of Applied Ecology,
Chinese Academy of Sciences, China

Michael Schlöter

German Research Center for Environmental Health
Germany
Xuejun Wang
Peking University, China
Lizhong Zhu
Zhejiang University, China

Atmospheric environment

Jianmin Chen
Fudan University, China
Abdelwahid Mellouki
Centre National de la Recherche Scientifique
France
Yujing Mu
Research Center for Eco-Environmental Sciences,
Chinese Academy of Sciences, China
Min Shao
Peking University, China
James Jay Schauer
University of Wisconsin-Madison, USA
Yuesi Wang
Institute of Atmospheric Physics,
Chinese Academy of Sciences, China
Xin Yang
University of Cambridge, UK

Environmental biology

Yong Cai
Florida International University, USA
Henner Hollert
RWTH Aachen University, Germany
Jae-Seong Lee
Hanyang University, South Korea
Christopher Rensing
University of Copenhagen, Denmark
Bojan Sedmak
National Institute of Biology, Ljubljana
Lirong Song
Institute of Hydrobiology,
the Chinese Academy of Sciences, China
Chunxia Wang
National Natural Science Foundation of China
Gehong Wei
Northwest A & F University, China
Daqiang Yin
Tongji University, China
Zhongtang Yu
The Ohio State University, USA

Environmental toxicology and health

Jingwen Chen
Dalian University of Technology, China
Jianying Hu
Peking University, China
Guibin Jiang
Research Center for Eco-Environmental Sciences,
Chinese Academy of Sciences, China
Sijin Liu
Research Center for Eco-Environmental Sciences,
Chinese Academy of Sciences, China
Tsuyoshi Nakanishi
Gifu Pharmaceutical University, Japan
Willie Peijnenburg
University of Leiden, The Netherlands
Bingsheng Zhou
Institute of Hydrobiology,
Chinese Academy of Sciences, China

Environmental catalysis and materials

Hong He
Research Center for Eco-Environmental Sciences,
Chinese Academy of Sciences, China
Junhua Li
Tsinghua University, China
Wenfeng Shangguan
Shanghai Jiao Tong University, China
Yasutake Teraoka
Kyushu University, Japan
Ralph T. Yang
University of Michigan, USA

Environmental analysis and method

Zongwei Cai
Hong Kong Baptist University,
Hong Kong, China
Jiping Chen
Dalian Institute of Chemical Physics,
Chinese Academy of Sciences, China
Minghui Zheng
Research Center for Eco-Environmental Sciences,
Chinese Academy of Sciences, China

Municipal solid waste and green chemistry

Pinjing He
Tongji University, China
Environmental ecology
Rusong Wang
Research Center for Eco-Environmental Sciences,
Chinese Academy of Sciences, China

Editorial office staff

Managing editor Qingcai Feng
Editors Zixuan Wang Suqin Liu Zhengang Mao
English editor Catherine Rice (USA)

JOURNAL OF ENVIRONMENTAL SCIENCES

环境科学学报(英文版)
(<http://www.jesc.ac.cn>)

Aims and scope

Journal of Environmental Sciences is an international academic journal supervised by Research Center for Eco-Environmental Sciences, Chinese Academy of Sciences. The journal publishes original, peer-reviewed innovative research and valuable findings in environmental sciences. The types of articles published are research article, critical review, rapid communications, and special issues.

The scope of the journal embraces the treatment processes for natural groundwater, municipal, agricultural and industrial water and wastewaters; physical and chemical methods for limitation of pollutants emission into the atmospheric environment; chemical and biological and phytoremediation of contaminated soil; fate and transport of pollutants in environments; toxicological effects of terrorist chemical release on the natural environment and human health; development of environmental catalysts and materials.

For subscription to electronic edition

Elsevier is responsible for subscription of the journal. Please subscribe to the journal via <http://www.elsevier.com/locate/jes>.

For subscription to print edition

China: Please contact the customer service, Science Press, 16 Donghuangchenggen North Street, Beijing 100717, China. Tel: +86-10-64017032; E-mail: journal@mail.sciencep.com, or the local post office throughout China (domestic postcode: 2-580).

Outside China: Please order the journal from the Elsevier Customer Service Department at the Regional Sales Office nearest you.

Submission declaration

Submission of an article implies that the work described has not been published previously (except in the form of an abstract or as part of a published lecture or academic thesis), that it is not under consideration for publication elsewhere. The submission should be approved by all authors and tacitly or explicitly by the responsible authorities where the work was carried out. If the manuscript accepted, it will not be published elsewhere in the same form, in English or in any other language, including electronically without the written consent of the copyright-holder.

Submission declaration

Submission of the work described has not been published previously (except in the form of an abstract or as part of a published lecture or academic thesis), that it is not under consideration for publication elsewhere. The publication should be approved by all authors and tacitly or explicitly by the responsible authorities where the work was carried out. If the manuscript accepted, it will not be published elsewhere in the same form, in English or in any other language, including electronically without the written consent of the copyright-holder.

Editorial

Authors should submit manuscript online at <http://www.jesc.ac.cn>. In case of queries, please contact editorial office, Tel: +86-10-62920553, E-mail: jesc@263.net, jesc@rcees.ac.cn. Instruction to authors is available at <http://www.jesc.ac.cn>.

Journal of Environmental Sciences (Established in 1989)

Vol. 26 No. 3 2014

Supervised by	Chinese Academy of Sciences	Published by	Science Press, Beijing, China
Sponsored by	Research Center for Eco-Environmental Sciences, Chinese Academy of Sciences		Elsevier Limited, The Netherlands
Edited by	Editorial Office of Journal of Environmental Sciences P. O. Box 2871, Beijing 100085, China Tel: 86-10-62920553; http://www.jesc.ac.cn E-mail: jesc@263.net , jesc@rcees.ac.cn	Distributed by	
		Domestic	Science Press, 16 Donghuangchenggen North Street, Beijing 100717, China Local Post Offices through China
		Foreign	Elsevier Limited http://www.elsevier.com/locate/jes
Editor-in-chief	Hongxiao Tang	Printed by	Beijing Beilin Printing House, 100083, China
CN 11-2629/X	Domestic postcode: 2-580		Domestic price per issue RMB ¥ 110.00

ISSN 1001-0742

